Dynamics and Orientation Ordering of Water in Lyotropic Liquid Crystals Using ^{2}H Double Quantum Filtered NMR Spectral Analysis

Chi-Yuan Cheng (鄭啓遠) and Lian-Pin Hwang* (黃良平)
Department of Chemistry, National Taiwan University, and Institute of Atomic and Molecular Sciences, Academia Sinica, Taipei, R.O.C.

The alignment of lyotropic liquid crystals in a magnetic field has been studied by line shape analysis of the T_1 process and 2D ^{2}H double quantum filtered (DQF) NMR to investigate water dynamics and orientational feature in Cetyltrimethylammonium bromide (CTAB)/Sodium Salicylate (NaSal)/D_2O liquid crystals. The same system but in powder form was also examined. In the ordered liquid-crystalline phase, the single quantum line shapes showed splitting of doublets due to the residual quadrupolar interaction, while the double quantum spectra observed splitting patterns with damped oscillation. The modified cone model is invoked to describe the restricted motions of bound D_2O molecules. Ten to thirteen bound water molecules are found to associate with each CTAB molecule and the correlation time of wobbling motion of the bound water is in the time scale of 10^{-8} s. At 10 °C, the motional correlation times of water in the powder sample have the same magnitude as those in the oriented sample. This study shows that the analysis of DQF relaxation spectra provides a more detailed source of motional information than the normally used measurements.

INTRODUCTION

Cetyltrimethylammonium bromide (CTAB) is a cationic surfactant containing aliphatic hydrocarbon chains. It forms a lyotropic liquid-crystalline phase at the concentration above 20% (0.68 mol/kg) at room temperature.[1] It is well-known that lyotropic liquid crystals can be aligned in a magnetic field.[2-5] The rod-like micelles in the CTAB/D_2O system may orient with their principal axes parallel to the magnetic field for a type I hexagonal mesophase.[1-3] After adding sodium salicylate (NaSal) into this system, the insertion of a salicylate anion into a micelle accounts for the elongation of the CTAB micelle.[6] Subsequently, the orientation of the CTAB/NaSal micelle changes to a direction perpendicular to the magnetic field,[3] and the CTAB/NaSal/D_2O system yields a type II laminar mesophase.[7,8] If the CTAB/NaSal mesophase sample is prepared in the absence of a magnetic field, a powder pattern is observed as a result of the random orientation of the liquid-crys5talline domains.[2-5]

In the anisotropic liquid-crystalline domains, the nuclear quadrupole interaction of a spin-bearing molecule is not averaged to zero. Thus, in the usual single quantum (SQ) spectrum, a solid like quadrupolar splitting ($\Delta\nu_q$) accounts for the presence of preferential orientation of a spin-bearing molecule, which results in the persistence of residual quadrupolar interaction. It is believed that quadrupolar splitting for an aligned liquid-crystalline sample is given by $\langle\Delta\nu_q\rangle \propto \frac{1}{2}\langle 3\cos^2\theta' - 1\rangle$, where θ' is the angle between the principal axis of quadrupolar interaction and the magnetic field.[2-5] Here, the notation $\langle ... \rangle$ means taking the average over the orientational distribution of θ' in liquid-crystalline domains. Therefore, quadrupolar splitting observed in a liquid-crystalline sample gives information on the orientation of the director of the mesophase.[2-9] But $\Delta\nu_q$ may be influenced by other factors, such as mobility and population of the spin-bearing molecules in the liquid-crystalline phase, and therefore, sometimes it may misjudge the orientation of the mesophase.[2,5]

The use of ^{2}H double quantum filtered (DQF) NMR spectroscopy as a diagnostic tool for the detection of anisotropy in a macroscopically disordered system has recently been developed.[10-13] In particular, for the I = 1 spin system, the double quantum coherence vanishes in the isotropic medium, and hence observation of the DQF spectra indicates the presence of the anisotropic motion of the spin-bearing molecules due to residual interaction. In this work, in addition to the usual investigation by T_1 line shape analysis, we employed DQF NMR spectroscopy to deduce the temperature-dependent water dynamics and orientational feature in the CTAB/NaSal/D_2O lyotropic liquid-crystalline systems. The

Dedicated to Professor Sheng-lieh Liu on the occasion of his ninetieth birthday.

* Corresponding author. Tel: +886-2-23668287; Fax: +886-2-23636359; E-mail: nmra@po.iams.sinica.edu.tw

results of the powder system are also examined.

THEORY

Two-Site Exchange Model with Residual Quadrupolar Interaction

The NMR relaxation model comprises two mutually exchangeable regions of water denoted as a "fast" site (site *f*) and a "slow" site (site *s*). The former water molecules refer to nonperturbed bulk molecules with zero averaging of quadrupolar interaction, whereas the latter are the hydration on the interface of the amphiphile.[3-5,9] In DQF NMR, the detectable signal is generated from the second rank tensor which is formed during the creation time of the DQF pulse sequence[10-13] $\pi/2\text{-}t_1/2\text{-}\pi\text{-}t_1/2\text{-}\pi/2\text{-}\tau\text{-}\pi/2\text{-}t_2$ (Acq.). The effect of this pulse sequence for spin-1 nuclei in a heterogeneous system is as follows. The first $\pi/2$ pulse transforms the Zeeman order T_{10} into single-quantum coherence T_{11} which then generates T_{21} in the creation time *via* the residual quadrupolar interaction. The π pulse is used as spin-echo to remove the field inhomogeneity. The second $\pi/2$ pulse with DQF phase cycling transforms T_{21} into double-quantum coherence T_{22}. Since τ is set to be 10 μs, the relaxation of T_{22} component may be neglected during time τ. The last $\pi/2$ pulse transforms the double-quantum coherence into an observable signal. In the present case, a representation of the molecular situation with exchange between a fast site *f* and a slow site *s*, characterized with a residual quadrupolar interaction, is needed. Hence, the evolution in the t_1 period of the related transverse components T_{11} and T_{21} at sites *f* and *s*, expressed by superscripts, may be described by the following rate equation of density matrix operators[10-11,14]

$$\frac{d}{dt}\begin{pmatrix} T_{11}^f \\ T_{21}^f \\ T_{11}^s \\ T_{21}^s \end{pmatrix} = \begin{pmatrix} -R_{11}^f - k_{fs} - \Delta & 0 & k_{sf} & 0 \\ 0 & -R_{21}^f - k_{fs} - \Delta & 0 & k_{sf} \\ k_{fs} & 0 & -R_{11}^s - k_{sf} + \Delta & -i\omega_{q,\theta} \\ 0 & k_{fs} & -i\omega_{q,\theta} & -R_{21}^s - k_{sf} + \Delta \end{pmatrix} \begin{pmatrix} T_{11}^f \\ T_{21}^f \\ T_{11}^s \\ T_{21}^s \end{pmatrix} \tag{1}$$

where $\omega_{q,\theta} \equiv \frac{1}{2}\omega_q(3\cos^2\theta - 1)$. $\omega_{q,\theta}$ and ω_q are the residual quadrupolar interactions in the laboratory frame and molecular frame, respectively. θ is the angle between the local symmetry axis of the quadrupolar interaction tensor and the Zeeman field. k_{fs} (k_{sf}) is the microscopic rate constant for transfer from site *f* (*s*) to site *s* (*f*), and $\Delta = \frac{1}{2}i\delta$. The chemical shift is denoted as δ, which is regarded as the difference between the chemical environments of the two sites.[3,15] In addition, the detailed balancing of the exchange process considers that $P_f k_{fs} = P_s k_{sf}$, where we define P_f and P_s as the total population in site *f* and site *s*, respectively. In Eq. (1), the spin relaxation rate constants for single and double quantum coherence (expressed by the first subscript of *R*) with different sites α (α= *f* or *s*) are given by $R_{11}^\alpha \equiv \frac{3}{160}\chi_\alpha^2(3J_0^\alpha + 5J_1^\alpha + 2J_2^\alpha)$ and $R_{21}^\alpha \equiv \frac{3}{160}\chi_\alpha^2(3J_0^\alpha + 5J_1^\alpha + 2J_2^\alpha)$,[14] where the quadrupolar coupling constants are $\chi_\alpha \equiv \frac{e^2Qq_\alpha}{\hbar}$. J_n^f and J_n^s are the spectral density functions defined below for motional relaxation of D_2O molecules in *f* and *s* sites, respectively.

Since the O-D bonding of the water molecule is considered to be cylindrical, the contribution of the asymmetry parameter of the electric field gradient to the relaxation is negligible. To guarantee the validity of this equation, the condition $\tau_{exe} >> \tau_c$ must hold, where τ_c represents the microscopic motional correlation times defined below, and τ_{exe} is defined as $\tau_{exe} = \frac{P_f}{k_{sf}} = \frac{P_s}{k_{fs}}$.

Spectral Density for Fast Motion Site

For a fast motion site the reorientational Brownian motion of water molecules averages the electric quadrupolar interaction experienced by the ^2H nucleus to zero. The spectral density function for fast sites is given by

$$J_n^f = \frac{2\tau_f}{1+(n\omega_0\tau_f)^2} \tag{2}$$

where τ_f is the effective reorientational correlation time of water molecules and ω_0 is the Larmor precession frequency of the deuteron.

Spectral Density for Slow Motion Sites

The spectral density functions for a slow site with consideration of residual quadrupolar interaction are defined by[14]

$$\begin{aligned} J_0^s &\equiv j_0^s(1+\tfrac{10}{7}\langle D_{00}^{(2)}\rangle + \tfrac{18}{7}\langle D_{00}^{(4)}\rangle - 5\langle D_{00}^{(2)}\rangle^2) \\ J_1^s &\equiv j_1^s(1+\tfrac{5}{7}\langle D_{00}^{(2)}\rangle - \tfrac{12}{7}\langle D_{00}^{(4)}\rangle) \\ J_2^s &\equiv j_2^s(1-\tfrac{10}{7}\langle D_{00}^{(2)}\rangle + \tfrac{3}{7}\langle D_{00}^{(4)}\rangle) \end{aligned} \tag{3}$$

where $D_{00}^{(n)}$ are the Wigner rotation matrix elements with the orientation relative to the laboratory frame, and $\langle ... \rangle$ means taking the average over space of motions not restricted by the binding interactions.

To describe the motions in the slow motion sites, the cone model of Brainard and Szabo is invoked,[16] but with a

simplified modification by leaving out the mode for overall reorientation in order to facilitate the calculation of the spectral density functions of the bound water molecule. The spectral density function is given by[17]

$$j_n^s = 2(d_{00}^2(\beta))^2 \frac{(1-S^2)[6D_w/(1-S^2)]}{[6D_w/(1-S^2)]^2+(n\omega_o)^2} + 4(d_{10}^2(\beta))^2 \left\{ \frac{S^2 D_i}{D_i^2+(n\omega_o)^2} + \frac{(1-S^2)[D_i+5D_w/(1-S^2)]}{[D_i+5D_w/(1-S^2)]^2+(n\omega_o)^2} \right\} + 4(d_{20}^2(\beta))^2 \left\{ \frac{4S^2 D_i}{(4D_i)^2+(n\omega_o)^2} + \frac{(1-S^2)[4D_i+2D_w/(1-S^2)]}{[4D_i+2D_w/(1-S^2)]^2+(n\omega_o)^2} \right\} \quad (4)$$

where $d_{mn}^2(\beta)$ are elements of reduced Wigner rotation matrix and β is the angle between the C_2 axis of a D_2O molecule and principal axis of residual quadrupolar interaction, i.e., O-D bond. In this case, we set $\beta = 54°$ since the plausible model for the interaction of water molecules with the surfactant is one in which the oxygen atom of the water molecules interactions with the positively charged head group of the surfactant.[7] One may believe that the internal rotation is around the C_2 axis of D_2O and the distributions C_2 orientation with respect to the director is within a cone. The distribution of the cone may be expressed by an order parameter S given by $S \equiv \langle D_{00}^{(2)} \rangle_s$, where the average is over the orientational distribution of water by taking into account the orientation variations due to the wobbling motion and also due to the available site arrangement of water to interact with the head groups of surfactant. Here in the case of $S = 0$ the bound water molecules have completely randomized orientational distribution and for $S = 1$ all the bound water aligns with a particular orientation. The internal rotation and wobbling motion of the D_2O have correlation times $\tau_i \equiv 1/(4D_i)$ and $\tau_w \equiv 1/(6D_w)$, respectively. Here, the internal rotation is presumably faster than the wobbling motion. These two motional correlation times are presumably larger than τ_f. With this model the second and third terms in Eq. (3) may be readily evaluated as $\langle D_{00}^{(2)} \rangle = SD_{00}^{(2)}(\theta)$ and $\langle D_{00}^{(4)} \rangle = \langle D_{00}^{(4)} \rangle_s \langle D_{00}^{(4)} \rangle(\theta)$ where axial symmetry of the binding interaction and site distribution are assumed. To evaluate the $\langle D_{00}^{(4)} \rangle_s$ term in terms of S, an isotropic distribution with the director of within a cone angle of b is invoked.[10,11] Brainard and Szabo obtained $S = \frac{1}{2}\cos b(1+\cos b)$.[16] We than yield $\langle D_{00}^{(4)} \rangle_s = (S/8)[28S-7(1+8S)^{1/2}+1]$. Hence, with this particular model one may evaluate the spectral density functions for site s.

The strength of binding interaction, in terms of residual quadrupolar interaction, depends on the nature of the bound water and the bound state. The position with maximum ω_q, denoted by ω_{qm}, may be defined as the D_2O molecule bound on the bound state with maximum strength of interaction. Thus, the quadrupolar interaction of D_2O gives $\omega_{qm} = \frac{3}{4}\chi_s$. Since both the S and ω_q parameters share the same degree of randomness after averaging over the same orientational distribution, one may relate S linearly with the residual quadrupolar anisotropy ω_q to $S \equiv \omega_q/\omega_{qm}$.

Calculation of Line Shape in the T_1 Process

Here we describe the use of the above theory in simulating the signal of the free induction decay after the inversion recovery pulse sequence (i.e., π-τ-$\pi/2$-Acq.). The total equilibrium state multipoles can be calculated from the corresponding density matrix elements as $T_{10,eq} \equiv \frac{\gamma\hbar B_0 I(I+1)}{3\sqrt{2}kT}$, where γ is gyromagnetic ratio, k is the Boltzmann constant, and B_0 is the Zeeman field.

Since we have exchanging species, the individual multipoles must be appropriately population weighted. The effects of the π pulse are then calculated, and thus immediately after the π pulse and including population weighting state multipoles as the initial condition before evolution of τ we have $T_{10}^f(0) = -p_f T_{10,eq}$ and $T_{10}^s(0) = -p_s T_{10,eq}$. Eq. (1) is also used for simulation of the single quantum spectrum. For the calculation of T_1, the evolution of the longitudinal magnetization during the delay time follows the rate equation[10,14]

$$\frac{d}{dt}\begin{pmatrix} T_{10}^f \\ T_{10}^s \end{pmatrix} = \begin{pmatrix} -R_{10}^f - k_{fs} & k_{sf} \\ k_{fs} & -R_{10}^s - k_{sf} \end{pmatrix} \begin{pmatrix} T_{10}^f \\ T_{10}^s \end{pmatrix} \quad (5)$$

where $R_{10}^f \equiv \frac{3}{160}\chi_f^2 (J_1^f + 4J_2^f)$, and $R_{10}^s \equiv \frac{3}{160}\chi_s^2 (J_1^s + 4J_2^s)$.

An isotropic distribution of θ is applied to simulate the situation of the random orientational distribution of liquid-crystalline systems in the powder sample. Then the signal of the longitudinal magnetization after the delay time τ can be evaluated as $M_z(\tau) \propto \int_0^\pi d\theta \sin\theta (T_{10}^f(\tau) + T_{10}^s(\tau))$. Furthermore, in the case of a fixed angle of θ, a Gaussian distribution $f(\theta')$ with a standard deviation of σ may be invoked to represent the contribution from the deviation of θ, i.e., $M_z(\tau) \propto \int_0^\pi d\theta' f(\theta')(T_{10}^f(\tau) + T_{10}^s(\tau))$.

EXPERIMENTAL

By stirring at elevated temperatures for 1 hr, 1.0 m CTAB (Acrôs, 99%) solution was prepared in D_2O (Cambridge Isotope Laboratories, 99%). Then, the required amount of NaSal (Merck) was added to the solution with CTAB/NaSal mole ratio of 1 to form a powder sample. For measuring a powder sample, the as-prepared sample was put into a mag-

netic field immediately after the preparation. The oriented samples were prepared by first heating the as-prepared sample in a magnetic field (11.75 T or 7.05 T) at a temperature higher than its isotropic temperature (~70 °C) for at least 1 hr, and then slowly cooling down to form the liquid-crystalline phase.

The ^{2}H NMR measurements were performed on Bruker MSL-500 and MSL-300 spectrometers operating at 76.78 MHz (11.75 T) and 46.07 MHz (7.05 T) with a 90° pulse of 30 μs and 20 μs, respectively. The T_1 relaxation measurements were obtained using the inversion recovery pulse sequence. DQF pulse sequence is the same as described in the previous section. 2D DQF data acquisitions involved the collection of 1K t_2 points and 256 incremented t_1 values. Only real parts of the spectra are displayed in this work and the spectral phase is referred to that of the corresponding SQ spectrum. A delay of at least 5 T_1 was allowed between scans for the T_1 and DQF spectra with proper phase cycling. The temperatures, calibrated with a methanol reference, were controlled within ± 0.5 °C.

RESULTS

The DQF signal of liquid-crystalline sample became vanishing small at temperatures above 40 °C. This indicated the transition from a liquid-crystalline phase into an isotropic phase where the motion of water molecules became more randomized and faster. Thus, a DQF experiment was inappropriate for measurements above this temperature. The appearance of liquid crystal showed turbid form at temperatures below 10 °C. It revealed that it is below the Krafft point.[2,5] Therefore, we limited our experiments to the temperature range of 10 ~ 30 °C for oriented samples. Furthermore, for a powdered form sample, we performed the measurement of the sample at 10 °C in order to avoid the re-alignment of liquid-crystalline domains in a magnetic field.

The trend of 1D DQF spectra in the oriented sample had a damped oscillation pattern with respect to creation time. That was completely different from the observation in the powder sample. The typical 1D DQF spectrum of the powder sample and the oriented sample are shown in Fig. 1. It was la-

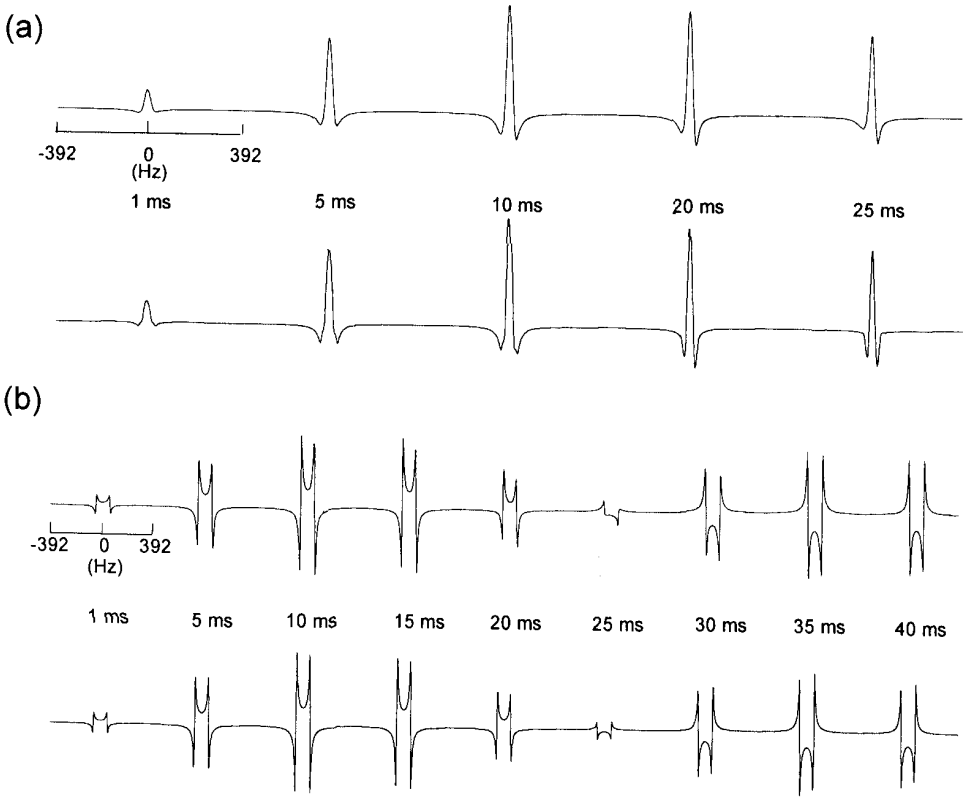

Fig. 1. Experimental (upper) and simulated (lower) 46.07 MHz ^{2}H 1D DQF spectra of CTAB/NaSal/ D_2O system for (a) powder sample and (b) oriented sample at 10 °C upper and 30 °C lower, respectively. The creation times are cited underneath the spectra. The splitting patterns shown in (b) are due to the coherent direction of residue quadrupolar interaction.

borious to analyze the 1D DQF spectra of the oriented sample because of long periodicity. Therefore, it is convenient to use 2D DQF spectral analysis to characterize water dynamics by Fourier transform of the signals from t_1 and t_2 to ω_1 space and ω_2 space.

Evaluation of χ_f and χ_s

The value of quadrupolar coupling constant for D_2O is an important issue while analyzing ^2H NMR relaxation data. Several measurements and theoretical calculations have demonstrated the quadrupolar coupling constant for the deuteron of D_2O in ice *Ih* and *VIII* phases.[18] Molecular dynamics simulation of liquid water indicated that its value usually varies with the geometry of D_2O and especially depends both on intra- and inter-molecular distance of D_2O.[19] It also indicated that the magnitude of quadrupolar coupling constant is in the range of 180 kHz to 373 kHz. Determined by nuclear quadrupole resonance, the values of quadrupolar coupling constant in ice are measured to be between 213 and 226 kHz.[20-22] Recently, many measurements in liquid D_2O have been published[18-22] and the values of quadrupolar coupling constants at room temperature are scattered over quite a large range (208~259 kHz). We assumed the deuteron quadruplar coupling constant of D_2O in a fast site to be χ_f = 222 kHz taken for liquid water,[23,24] and χ_s = 240 kHz taken for hydration water in barium carbonate[25] or in lithium sulfate[26] to mimic the situation of the bound waters in the environment of cationic surfactant.

Determination of $P_s\omega_q$

It is believed that the water molecules in phase II laminar liquid-crystalline domains are oriented with $\theta = 90°$.[9] It gives a quadrupolar interaction $\omega_{q\theta} = -\omega_q/2$ where $\omega_q = \frac{3}{4}\chi_s S$. If the micelle is randomly oriented in a magnetic field, the damped oscillation pattern of 1D DQF spectra vanishes (cf. Fig. 1a). Thus one may infer that the coherence of the residual quadrupolar interaction evolved during t_1 and t_2 periods is the cause for those observations. The experimental 2D DQF spectrum together with their corresponding simulation for the oriented sample at 30 °C is shown in Fig. 2.

In the fast exchange limit as compared with the frequency of residual quadrupolar interaction, i.e., $|\omega_{q\theta}\tau_{exe}| << 1$, we have $\tau_{exe} << |\omega_{q\theta}|^{-1} = 8 \times 10^{-3}$ *s*. Fig. 1b shows the experimental and the corresponding simulated 1D DQF spectra of liquid-crystalline sample to be within this limit. For the powder sample, there is no splitting pattern nor periodic oscillation found (see Fig. 1a). The oscillation in 1D spectra yields an offset resonance frequency in the 2D DQF spectra and the offset frequency corresponds to $P_s\omega_q$. It is equivalent to one half of the magnitude in $\Delta\nu_q$. To demonstrate the effect of exchange rate on spectral lines, the calculated results with various exchange rates are compared in Fig. 3. In the fast exchange limit, a coherent orientation of water molecules will give same offset both in F_1 and F_2 domains. The offset fre-

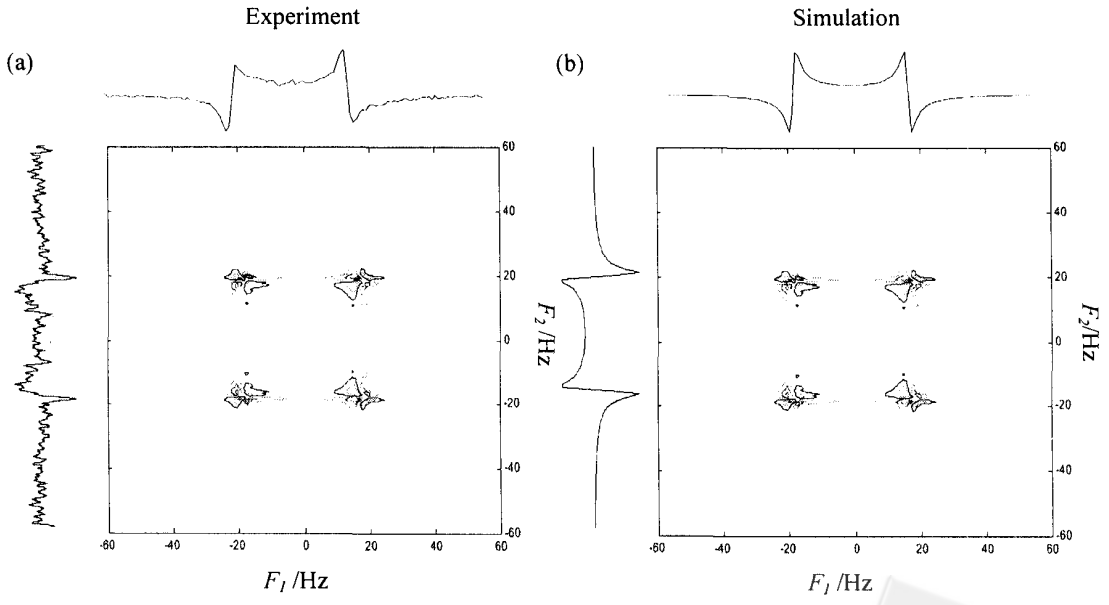

Fig. 2. Experimental (left) and simulated (right) contour plot of 46.07 MHz ^2H 2D DQF spectra for oriented sample at 30 °C. The dash line denotes negative intensity of DQF spectra.

quency forms a symmetric splitting pattern in 2D spectra. If the water molecules of the oriented sample are in a slow exchange region i.e., $|\omega_{q\theta}\tau_{exe}| \geq 1$, the offset resonance peaks merge into one peak (Fig. 3d). However, it is not the case for our experimental results.

Determination of τ_w from DQF Spectra

In the present study, ^{2}H DQF NMR spectra were obtained at 10 °C, 20 °C and 30 °C. The field-independent DQF spectra were found for all the samples studied. This sets a lower bound around 2 ns for τ_w. For a powder sample, a larger value of τ_w causes a faster decay of the DQF spectral peaks. The profile of the 1D DQF peak intensity with increasing creation time t_1 may be utilized in the determination of τ_w [10] Similarly, for an oriented sample, a slower τ_w causes a faster decay of DQF spectra within one period and also shortens the oscillation period. Usually, one finds that, with increasing τ_w, the line widths in F_2, domains are much broader than those in

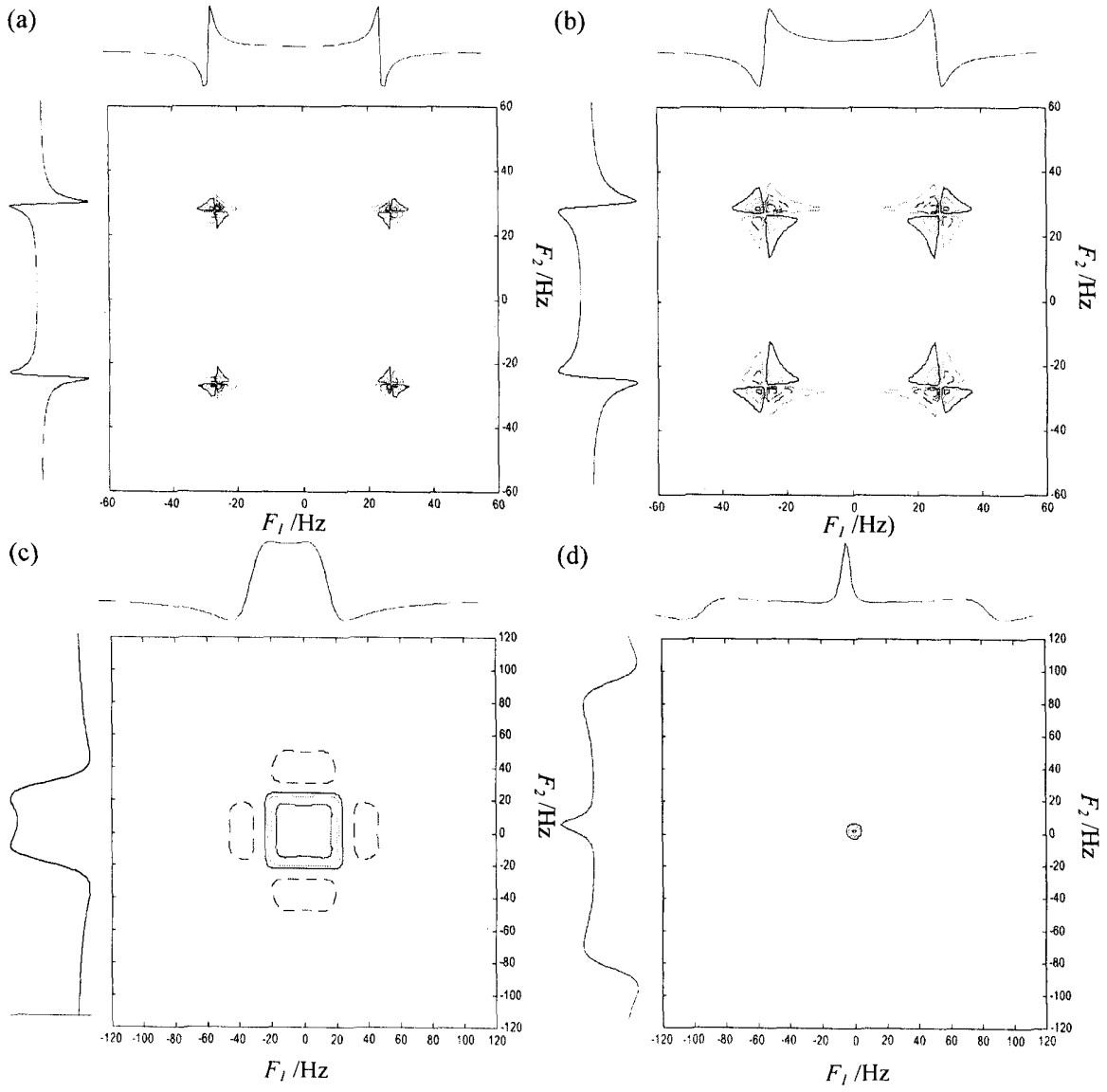

Fig. 3. 46.07 MHz 2D DQF contour plots simulation for (a) $\tau_{exe} = 10^{-5}$ *s*, $|\omega_{q\theta}\tau_{exe}| = 0.0017$, (b) $\tau_{exe} = 10^{-4}$ *s*, $|\omega_{q\theta}\tau_{exe}| = 0.0170$, (c) $\tau_{exe} = 10^{-3}$ *s*, $|\omega_{q\theta}\tau_{exe}| = 0.1696$, (d) $\tau_{exe} = 10^{-2}$ *s*, $|\omega_{q\theta}\tau_{exe}| = 1.6965$. The other parameters set as follow: $\tau_f = 1 \times 10^{-12}$ *s*, $\tau_l = 5 \times 10^{-12}$ *s*, $\tau_w = 10^{-8}$ *s*, $P_s = 0.3$, $S = 0.001$, $\theta = 90°$, $\sigma < 10^{-4}$. The dashed line denotes negative intensity of DQF spectra.

F_1 domains. All these features may be utilized in evaluating τ_w.

Determination of τ_{exe} from DQF Spectra

The splitting in the usual 1D spectrum is not always obvious to show the exchange feature. However, two-dimensional DQF NMR can be used to ascertain the effect of the exchange. As demonstrated in Fig. 3, the line shape of the cross peak provides direct information on the exchange lifetimes. The most informative range for recording 2D DQF spectra is under fast exchange conditions, $|\omega_{q\theta}\tau_{exe}| \leq 1$. For a slower exchange, the characteristic broadening and coalescence features appearing in the 2D plot may blur the analysis.

Determination of P_s and S

As described above, the value of P_sS may be estimated from $\Delta\nu_q$. Since the line width of SQ spectrum is more sensitive to S than to P_s, one can then estimate P_s and S separately. Along with other parameters obtained, 2D DQF spectra may be used to refine the values of P_s and S. Also, the splitting in the F_2 domain of the SQ spectra is obscured due to line broadening with the increase of S exceeding 0.002 but not effected with the increase of P_s. The obtained values of P_s and S are given in Table 1. Furthermore, the knowledge of P_s may be invoked to evaluate the number of bound water associated with CTAB molecules as will be discussed below.

Determination of τ_f and τ_i from Inversion Recovery Experiment

It was found that the calculated T_1 spectra are very sensitive to the choice of τ_f and τ_i. Since the field-independent T_1 spectra were found for all our samples, τ_f and τ_i may follow the motional narrowing conditions. Moreover, the line width of SQ spectra is rather sensitive to the variation of τ_i but not to the variation of τ_f. The SQ line width may be used to obtain τ_i and then the τ_f value may be determined from the T_1 fitting.

Fig. 4 show the typical ^2H spectra of D_2O in CTAB/NaSal liquid-crystalline phase from an inversion recovery experiment at 46.07 MHz. The line shapes were simulated with the parameters previously determined. Fine adjustment of the parameters has been made in order to fit the evolved spectra. The corresponding simulations are also shown in the figure. The consistency between experimental and calculated results is satisfactory. All the parameters used to calculate the simulated spectra at resonance frequencies 46.07 MHz are listed in Table 1.

Evaluation of δ and σ

The asymmetry in the SQ spectra was attributed to the difference in chemical shift between bound and free D_2O molecules.[3,15] Therefore, δ value is utilized to yield the asymmetry in the observed quadrupolar doublet.

The deviation (σ) of θ is invoked to deal with the degree of alignment for water orientations. The obtained σ value is negligible so that the bound water molecules are coherently oriented in a magnetic field.

DISCUSSION

In practice, when referring to interfaces of water with micelles one may find various complicated perturbation interactions of water. For simplicity, the division of water found in a micellar system into slow and fast components is quite conventional.[3-9] For quadrupolar nuclear systems, the bound states of hydration water are expressed in terms of residual quadrupolar interactions of deuterium nuclei. The advent of DQF NMR selectively excites the spin species possessing residual quadrupolar interaction. Therefore, the DQF NMR study of quadrupolar relaxation is helpful in deciphering the characteristics of hydration water. Since P_s, S, and τ_{exe} can be used to adjust the trend of damped oscillating pattern of DQF spectra, it is indicative that the damped oscillating pattern of DQF spectra is related to the feature of water in the bound state. Therefore, the DQF spectral analysis is particularly suitable for studying bound water on the interface of a

Table 1. The Parameters Used in the Fitting of T_1 and DQF Relaxation Spectra for (a) Powder Sample and (b) Oriented Sample ($\chi_f/2\pi$ = 222 kHz, $\chi_s/2\pi$ = 240 kHz)

	T (°C)	P_s	τ_f (s)	τ_i (s)	τ_w (s)	τ_{exe} (s)	S	δ (Hz)	σ
(a)	10	0.30	4.6×10^{-12}	8.5×10^{-11}	5.0×10^{-8}	2.0×10^{-4}	0.0015	2	-
(b)	10	0.24	4.5×10^{-12}	8.2×10^{-12}	5.0×10^{-8}	1.3×10^{-4}	0.0015	2	1*
	20	0.23	4.1×10^{-12}	8.0×10^{-12}	1.2×10^{-8}	1.2×10^{-4}	0.0012	1	1*
	30	0.20	3.0×10^{-12}	8.0×10^{-12}	1.0×10^{-8}	1.0×10^{-4}	0.0010	1	1*

* $\theta = 90°$ (10% error in all parameters)

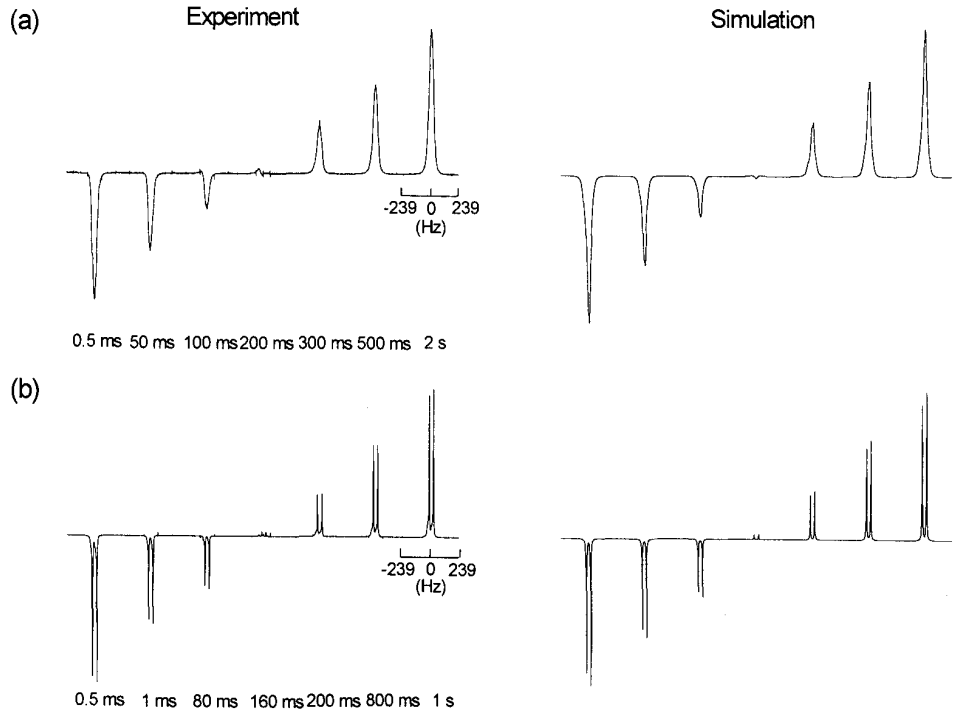

Fig. 4. Experimental (left) and simulated (right) 46.07 MHz ^{2}H spectra of inversion recovery experiments for (a) powder sample and (b) oriented sample at 10 °C and 30 °C, respectively. The delay times after inversion pulse are cited underneath the spectra.

micelle.

Effects of temperature and mesophase orientation

As shown in Fig. 5, the quadrupolar splitting increases with decreasing temperature in CTAB/NaSal laminar phase. Also, as concentrations of CTAB increase, the quadrupolar splitting and line width tends to increase. It is believed that the increase of P_s and S may account for the increased splitting. However, the splitting was not properly interpreted in previous studies.[3,9] In the present work, we provide some quantitative information on P_s and S as listed in Table 1. It is shown that P_s and S increase with decreasing temperature, e.g. at lower temperatures both the number and order of bound water increase. The smallness of S represents to a large extent the fluctuation of the director motions. Also, a small variation of director's direction, represented by σ, indicates that all directors of liquid-crystalline domains ion align coherently.

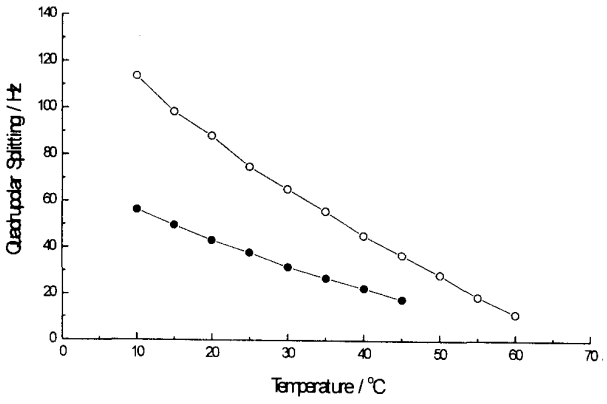

Fig. 5. Variation of quadrupolar splitting with temperature in CTAB/NaSal/D_2O liquid-crystalline system. (CTAB/D_2O = 1.2 m, CTAB/NaSal mole ratio = 1 (●); CTAB/D_2O = 1 m, CTAB/NaSal mole ratio = 1 (○)).

In the temperature range of mesophase studied, the dynamics of water is in the fast exchange regime. The exchange lifetime from our measurement is about 1.0×10^{-4} s. The magnitude is in good agreement with Rapp's results studied from SQ line shape analysis,[3] but contradictory to Rapp's observation, our results yield a normal trend with respect to temperature, i.e., the exchange lifetimes ranging from 1.3×10^{-4} to 1.0×10^{-4} s with the increase of temperature from 10 to 30 °C are

observed. In Table 1, it shows that the exchange lifetime for the powder sample is found to be larger than the one for the oriented sample. A larger lifetime at a site signifies a larger site population or/and a slower exchange rate.

At 10 °C, the motional correlation times, τ_f, τ_i and τ_w, of water in the powder sample have the same magnitude as those in the oriented sample. However, the water populations in these two systems are distinct. P_s has a smaller magnitude in the oriented sample than in a random powder sample. One may infer that, in the latter system, the inter-domain region of randomly staggered domains of a liquid-crystalline system may create more similar caging sites for hydration water to associate with CTAB molecules.

Characteristics of water motions

The reorientational correlation times τ_f of D_2O in a fast site are expected to be the same as those in the bulk. Indeed, the results are consistent with the reorientational correlation times of bulk water measured from NMR[23,27] and dielectric relaxation[28] studies. The rotational correlation times of water molecules around the C_2 axis, the τ_i values, are about 8.0×10^{-12} s in a CTAB/NaSal type II mesophase. The results are twice as slow as those found in a type I sample of CTAB/D_2O[24] and alkylammonium chloride (C_nTAC)/D_2O[29,30] system. Nevertheless, the temperature independent behavior of the τ_i process indicates that the environment of internal rotation presents a negligible barrier for bound water, but their wobbling motions are in the order of 10^{-8} s and show strong temperature dependence. Furthermore, it is noted that the same magnitude of τ_w and S are observed in the oriented sample and in the powder sample at 10 °C (Table 1). All the evidence reflects the cooperative effect of the director motion only confined within a liquid-crystalline domain. Moreover, the reorientational correlation time of the methyl group of C_nTAB in $C_{16}TAB$/NaSal[31] and $C_{16}TAC$[32] mesophase are about 10^{-6} and 10^{-9} s, respectively. It shows that the $C_{16}TAB$/NaSal mesophase is more rigid and stiff than the $C_{16}TAC$ mesophase because of NaSal bridges between the CTAB micelle. Therefore, in accordance with all those results, the tumbling of a micelle is less apparent in a type II liquid-crystalline phase.

Estimation of the number of bound water on CTAB surfactant

Recent relaxation measurements have been used to evaluate the amount of bound water on a surfactant.[29,30] It was found that $n \leq 12$ in the main hydration water shell of lecithin, which is similar to CTAB conformation.[33] Moreover, using T_1 and self-diffusion measurements, Canet and co-worker estimated the number (n) of D_2O molecules bound to CTAB surfactant molecule in a micelle to be equal to 10.[24]

In this work, the number of bound water molecules per CTAB surfactant molecule n can be calculated from the slow site population P_s. In brief, the population of bound water is given by $P_s = [D_2O]_s/[D_2O]_t$, where $[D_2O]_t$ denotes the molar concentration of water in the system, and $[D_2O]_s$ denotes the molar concentration of water in the slow sites. Since we have [CTAB] = 1 m and in aqueous solution $[D_2O]_t$ = 50 m, the number of water molecules per surfactant molecule can be obtained with the help of the relation $n = \frac{[D_2O]_s}{[CTAB]} = \frac{P_s[D_2O]_t}{[CTAB]}$. Thus as listed in Table 2, in the temperatures from 10 °C to 30 °C, the number of water molecules associated with CTAB in a liquid-crystalline micelle varies from 10 to 13 water molecules per CTAB. Our results are consistent with those measurements of a type I liquid-crystalline phase. These results indicate the hydration number of CTAB remains the same either in a type I or in type II liquid-crystalline phase. Hence one may conclude that there is almost no morphological change for water associated with CTAB in the two different oriented micellar systems.

CONCLUSION

The water dynamics on the interface of a micelle is expected to be complicated. These phenomena are treated within the scope of two-site approximation. In the present study, the model comprises a "slow" anisotropic site involved in exchange with the "fast" bulk water. In an oriented sample, one may observe the quadrupolar splitting due to residual quadrupolar interaction. The degree of splitting depends on the population of water in an anisotropic region, quadrupolar coupling constant, order parameter, and exchange rates. It is believed that water molecules in the slow bound site of the oriented sample tended to orient in the magnetic field. The directors for the fluctuation of C_2 axes of water molecules in the bound state of CTAB/NaSal/D_2O mesophase are perpendicular to the magnetic field. In addition to the usual NMR

Table 2. The Number (n) of Bound Water on CTAB Surfactant at Various Temperatures

Sample	Temperature (°C)	$\Delta\nu_q$ (Hz)	P_s	n
Powder sample	10	-	0.30	15
Oriented sample	10	64	0.24	12
	20	48	0.23	12
	30	38	0.20	10

method, we applied DQF spectral analysis to attain more dynamical information in the oriented medium. This method also enables the interpretation of D_2O binding data in liquid-crystalline phase and allows more accurate determination of motional correlation times, which are too complicated for the application of the usual methods.

ACKNOWLEDGMENT

This work was supported by the National Science Council of the Republic of China under Grant No. NSC 89-2113-M-002-003.

Received September 7, 2001.

Key Words

2D DQF NMR; Dynamics; Lyotropic liquid crystal; CTAB.

REFERENCES

1. Wolff, T.; von Bünau, G. *Ber. Bunsenges. Phys. Chem.* **1984**, *88*, 1098.
2. Forrest, B. J.; Reeves, L. W. *Chem. Rev.* **1981**, *1*, 81.
3. Rapp, A.; Ermolaev, K.; Fung, B. M. *J. Phys. Chem. B* **1999**, *103*, 1705.
4. Robin-Lherbier, B.; Canet, D.; Marchal, J. P.; Brondeau, J. In *Solution Chemistry of Surfactants*; Mittal, K. L.; Lindman, B., Eds.; Plenum: New York, 1984; p 79.
5. Halle, B.; Furó, I. In *Phase Transitions in Complex Fluids*; Tolédano, P.; Figueiredo Neto, A. M., Eds.; World Scientific: Singapore, 1998; p 81.
6. Manohar, C.; Rao, U. R. K.; Valaulikar, B. S.; Iyer, R. M. *J. Chem. Soc., Chem. Commun.* **1986**, *4*, 379.
7. Hakala, M. R.; Wong, T. C. *Langmuir* **1986**, *2*, 83.
8. Guo, W.; Wong, T. C. *Langmuir* **1987**, *3*, 537.
9. Capitani, D.; Casieri, C.; Brigani, G.; La Mesa, C.; Segre, A. L. *J. Phys. Chem. B* **1999**, *103*, 6088.
10. Chen, Y. H.; Hwang, L. P. *J. Phys. Chem. B* **1999**, *103*, 5070.
11. Yu, T. Y.; Cheng, C. Y.; Hwang, D. W.; Huang, H. W.; Hwang, L. P. *Appl. Magn. Reson.* **2000**, *18*, 435.
12. Sharf, Y.; Eliav, U.; Shinar, H.; Navon, G. *J. Magn. Reson. B* **1995**, *107*, 60.
13. Shinar, H.; Seo, Y.; Navon, G. *J. Magn. Reson.* **1997**, *129*, 98.
14. Jacobsen, J. P.; Bildsøe, H. K.; Schaumburg, K. *J. Magn. Reson.* **1976**, *23*, 153.
15. Westlund, P.-O. *J. Phys. Chem. B* **2000**, *104*, 6059.
16. Brainard, J. R.; Szabo, A. *Biochemistry* **1981**, *20*, 4618.
17. Wong, T. C.; Wang, P. L.; Duh, D. M.; Hwang, L. P. *J. Phys. Chem.* **1989**, *93*, 1295.
18. Cummins, P. L.; Bacskay, G. B.; Hush, N. S. *Mol. Phys.* **1987**, *61*, 795.
19. Eggenberger, R.; Gerber, S.; Huber, H.; Searles, D.; Welker, M. *J. Chem. Phys.* **1982**, *97*, 5898.
20. Woessner, D. E. *J. Chem. Phys.* **1964**, *40*, 2341.
21. Lee, Y.; Jonas, J. *J. Chem. Phys.* **1972**, *57*, 4233.
22. Lang, E. W.; Lüdemann, H. D.; Piculell, L. *J. Chem. Phys.* **1984**, *81*, 382.
23. Halle, B.; Wennerström, H. *J. Chem. Phys.* **1981**, *75*, 1928.
24. Belmajdoub, A.; Boubel, J. C.; Canet, D. *J. Phys. Chem.* **1989**, *93*, 4844.
25. Chiba, T. *J. Chem. Phys.* **1963**, *39*, 947.
26. Ketudat, S.; Pound, R. V. *J. Chem. Phys.* **1957**, *26*, 708.
27. Nakahara, M.; Wakai, C. *J. Mol. Liq.* **1995**, *65*, 149.
28. Grant, E. H.; Shack, R. *J. Chem. Soc., Faraday Trans.* **1969**, *65*, 1519.
29. Halle, B.; Carlström, G. *J. Phys. Chem.* **1981**, *85*, 2142.
30. Bozonnet-Frenot, M. P.; Marchal, J. P.; Canet, D. *J. Phys. Chem.* **1987**, *91*, 89.
31. Hwang, L. P.; Wang, P. L.; Wong, T. C. *J. Phys. Chem.* **1988**, *92*, 4753.
32. Söderman, O.; Heriksson, U.; Olsson, U. *J. Phys. Chem.* **1987**, *91*, 116.
33. Finder, E. G. *J. Chem. Soc., Faraday Trans. II.* **1973**, *69*, 1590.